processes

MDPI

Article

Bacterial-Retted Hemp Fiber/PLA Composites

Lee M. Smith [1,2], Yu Fu [3], Raj Kumar Pittala [4], Xun Wang [5], Chloe Jabel [6,†], Kelvin Masignag [5,†], Josue Arellanes [5,†], Mahan Ghosh [5], Sheldon Q. Shi [5,*], Melanie Ecker [4] and Cuicui Wang [2]

[1] Department of Physical Sciences, Northeastern State University, 611 N. Grand Ave, Tahlequah, OK 74464, USA; smith819@nsuok.edu
[2] Z&S Tech, LLC, 202 Wellington Oaks CT, Denton, TX 76210, USA; ccw2730@gmail.com
[3] Leslie A. Rose Department of Mechanical Engineering, South Dakota School of Mines & Technology, 501 E. Saint Joseph Street, Rapid City, SD 57701, USA; yu.fu@sdsmt.edu
[4] Department of Biomedical Engineering, University of North Texas, 3940 N. Elm Street, Denton, TX 76207, USA; rajkumarpittala@my.unt.edu (R.K.P.); melanie.ecker@unt.edu (M.E.)
[5] Department of Mechanical Engineering, University of North Texas, 3940 N. Elm Street, Denton, TX 76207, USA; xunwang@my.unt.edu (X.W.); kelvinnelsonmasinag@my.unt.edu (K.M.); josuearellanes@my.unt.edu (J.A.); mahanghosh@my.unt.edu (M.G.)
[6] Department of Material Science and Engineering, University of North Texas, 3940 N. Elm Street, Denton, TX 76207, USA; chloejabel@my.unt.edu
* Correspondence: sheldon.shi@unt.edu
† These authors contributed equally to this work.

Abstract: The push for sustainability in all facets of manufacturing has led to an increased interest in biomass as an alternative to non-renewable materials. Hemp bast fiber mats were produced from a bacterial retting process, named BFM, as the fiber reinforcement. The objective of this study was to evaluate the feasibility of laminating BFM with polylactic acid (PLA) for a composite panel product. Since both BFM and PLA are biodegradable, the resulting BFM-PLA composites will be 100% biodegradable. PLA pallets were processed into thin polymer sheets which served as the matrix. The BFM and PLA plates were laminated in five layers and compression-molded into composite panels. Experiments were conducted on the three BFM-to-PLA ratios (35/65, 45/55, and 50/50). Mechanical properties (tensile and bending properties) and physical properties (thickness swell and water absorption) were tested and compared to the currently commercial sheet molding compound (SMC) from fiber glass. The thermal behavior of the BFM/PLA composites was characterized using dynamic mechanical analysis (DMA) and differential scanning calorimetry (DSC). The developed BFM/PLA composite product is a sustainable alternative to existing synthetical fiber-reinforced polymer (FRP) that is biodegradable in landfill at the end of life.

Keywords: PLA; hemp; bacterial retting; natural fiber composite; biodegradable

Academic Editors: Pedro Fernandes and Carla C. C. R. de Carvalho

Received: 30 January 2025
Revised: 3 March 2025
Accepted: 18 March 2025
Published: 27 March 2025

Citation: Smith, L.M.; Fu, Y.; Pittala, R.K.; Wang, X.; Jabel, C.; Masignag, K.; Arellanes, J.; Ghosh, M.; Shi, S.Q.; Ecker, M.; et al. Bacterial-Retted Hemp Fiber/PLA Composites. *Processes* **2025**, *13*, 1000. https://doi.org/10.3390/pr13041000

1. Introduction

The demand for lighter, energy-efficient, and more environmentally friendly materials has continued to increase. Early motor vehicles were motor-powered wood wagons. As technology progressed, the heavy use of metal became common. With the advances in polymer science and the need to reduce vehicle weight, polymers began to play an important role in modern vehicle design. Currently, many fiber-reinforced polymers (FRPs) are made from synthetic fibers, such as glass fiber, carbon fiber, and petroleum-based matrices, such as polypropylene, polyurethane, polycarbonate, and polyethylene. These materials are non-renewable, presenting a problem when the material reaches the end of life.

In recent years, there has been a push for more ecofriendly alternatives to synthetic fibers, using natural fibers as reinforcements and biodegradable resins as polymer matrices. Natural fiber sources are sisal, flax, rattan, bamboo, jute, kenaf, etc. Hemp (*Cannabis sativa* L.) has become popular because of its high cellulose content and high fiber strength [1,2]. Hemp bast fiber is a popular source in the textile industry.

Retting is the essential process to obtain high-quality lignocellulosic fibers. Dew, water, enzymatic, bacterial, chemical, and mechanical modes are the major types of retting processes [3]. While chemical retting can be faster and more controlled than the traditional water and dew retting, it requires the careful management of chemicals to minimize the high cost of chemicals and environmental impact. Bacterial and enzymatic retting utilize certain microorganisms and their products to break down the non-fiber components (pectin and lignin) that hold the cellulosic fiber together. The isolation and purification of enzymes or bacteria is an expensive process; therefore, the cost of enzymatic or bacterial retting alone is high. It is not economical to apply enzymes or certain bacterial strains to each batch of retting, especially for large-scale industrial applications. Fu et al. noted that the use of a small amount of pectinase (1% w/v) as a trigger had a significant effect on bacterial community succession and raised the possibility of using recycled retting solutions [4]. This strategy avoids the expensive and complex bacterial culture process, and enzyme-triggered self-cultured bacteria have been found to be very effective in natural fiber retting. The results of the life cycle assessment (LCA) of the retting process showed that the self-cultured bacterial retting process had 20–25% lower environmental impact than that the chemical and high-temperature processes [4,5].

Polylactic acid (PLA) is a biodegradable polymer derived from the fermentation of starches and sugars found in various crops including corn, sugar cane, and potatoes [6]. PLA is a thermoplastic aliphatic polyester polymer, made up of multiple lactic acid monomers with a carboxylic acid group on one end and a hydroxyl group at the other end of the polymer chain [7].

PLA has drawn attention as an alternative to the conventional petroleum-based thermoplastic polymers such as polypropylene (PP) and polyethylene (PE) [6].

Since both bast fibers from hemp and PLA are biodegradable, the resulting hemp/PLA composites will be 100% biodegradable. As shown in Figure 1, the methyl groups in the lactic acid monomers make up the PLA. Glucose is an anhydroglucose unit in the cellulose of hemp [8] (Figure 1). Each individual unit of the cellulose possesses three hydroxyl groups which could form an intermolecular hydrogen bond [9].

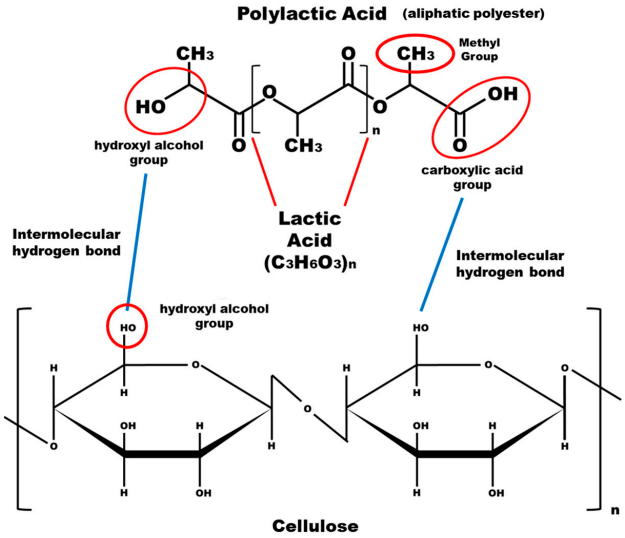

Figure 1. PLA and cellulose chemical structure and bonding.

Various processing techniques have been used to make hemp/PLA composites including injection molding, compression molding, melt blending, extrusion, and fusion deposition modeling (FDM) [10–14]. For many of these processes, the maximum amount of hemp fiber was reported as 30%wt due to the limitations of the processing method.

In this research, the self-cultured bacterial-retted fibers from hemp were formed into a fiber mat (BFM) and laminated with the PLA sheet. The incorporation of BFM into the PLA potentially improves the thermal behavior of composites. The performances of the resulting composites were evaluated in terms of their physical, mechanical, and thermal properties.

2. Materials and Methods

The hemp fibers were provided by HD Innovates LLC, Frisco, TX, USA. The polymer matrix was purchased from the distributor Filabot, Barre, VT, USA. The polymers were NatureWorks Ingeo™ (Plymouth, MN, USA) Biopolymer 4043D white PLA pellets.

2.1. Hemp Mat Forming

A small amount of hemp fiber was immersed in 40 °C water with 1% (*w*/*v*) pectinase for three days to obtain a solution with Bacillaceae bacteria present within it, which is the result of the enzymatic culturing [4]. The hemp fiber for mat manufacturing was cut to ¼ inch before retting with the bacterial solution for 3 days. The obtained retted fibers were magnetically stirred for one hour (500 rpm) before transferring to a mat-forming frame (16.5 cm × 10.2 cm) to be formed into a mat. The mats were then dried overnight at 80 °C for the next phase of composite fabrication.

2.2. PLA Sheet Forming

A single layer of PLA pellets was placed in a baking tray, which was placed on a heating plate at a temperature of 204 °C for 30 min, and a lid was placed on the baking tray to allow for effective heat transfer. Once the PLA was melted, the tray was removed from the heating plate and the lid was removed, allowing for the plate to cool.

The PLA plates were placed between two aluminum platens, which were placed into a DAKE hot press at a temperature of 204 °C, where a force of 5.5 kPa (1 metric ton) was applied for 5 min to allow the PLA to melt. After 5 min, the pressure was increased to 27.3 kPa (5 metric tons) to form a PLA sheet.

Aluminum spacers with three thicknesses (no spacer, 0.5 mm, and 1.0 mm) were used to control the PLA sheet thickness. The PLA sheets were cut into 16.5 cm × 10.2 cm sheets to fit into the composite mold.

2.3. BFM/PLA Panel Hot Pressing

A 5-layer laminate lay-up was chosen for the BFM/PLA composites (3 layers of BFM and 2 layers of PLA sheets; Figure 2).

The percentage of initial PLA content was increased by using PLA sheets with increasing thickness for each sample group, while the content of the BFM was kept the same. The upper and lower layers of the BFM were thinner than the middle layer of the BFM to allow for better PLA penetration during pressing.

Three separate hemp/PLA ratios were used, as shown in Table 1.

The layers of the laminate were placed within the aluminum mold, where two layers of wax paper were placed on the top and bottom of the layers for mold release. A hydraulic hot press was heated to a set temperature of 204 °C. The mold was placed within the hot press and a pressure of 5.5 kPa was applied for 10 min to allow for the core PLA layer in the lay-up to reach its melt temperature. The pressure applied to the mold was then raised to 54.6 kPa over a period of 20 min at a rate of 2.7 kPa/min in order to allow for the PLA

matrix to penetrate and permeate through the BFM. Once the designated pressure was reached, the press was turned off and cooled by circulating water through it for 30 min.

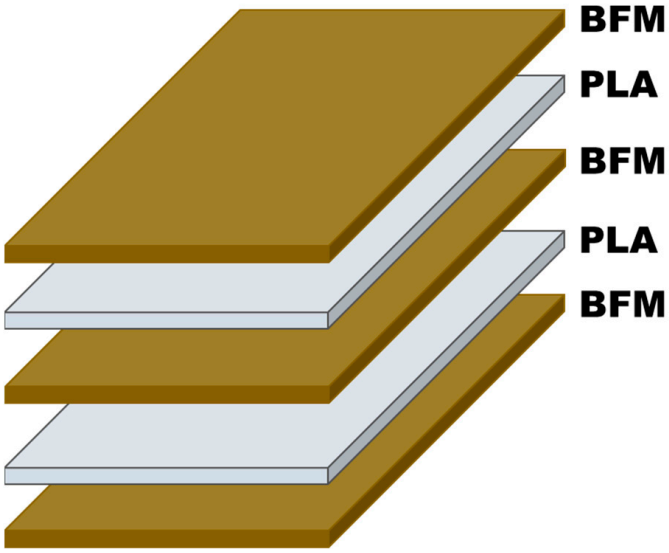

Figure 2. Five-layer hemp/PLA composite laminate structure.

Table 1. Initial and final BFM/PLA ratios.

Samples	Initial Ratios (%)		Final Ratios (%)		PLA Mass Loss (%)	Density g/cm^3
	BFM	PLA	BFM	PLA		
1 (BFM/PLA 53/47)	52.9	47.2	54.1	45.9	2.3	1.23
2 (BFM/PLA 43/57)	42.5	57.5	50.5	49.5	14.4	1.30
3 (BFM/PLA 35/65)	35.2	64.8	48.1	51.9	26.8	1.26

2.4. Property Testing

The tensile properties were tested in accordance with ASTM standard D3039 [15]. The bending properties were tested in accordance with ASTM standard D7264 [16]. Each composite panel was cut into 4 strips for both tensile and bending testing (2 strips used for each property, with 1 from the outside of the sample and 1 from the inside). The 24 mm by 1.5 mm tensile test samples were tested using a gauge length of 100 mm. The 8 mm by 1.5 mm bending samples were tested using a span of 60 mm. A Shimadzu AGSX universal testing machine with a load cell capacity of 10 kN was used for the tests.

2.5. Water Absorption (WA) and Thickness Swell (TS) Testing

WA and TS testing was conducted in accordance with the procedure described in ASTM D1037-12 [17]. The dimensions of the test sample were 25.4 mm × 25.4 mm × 1.5 mm. The initial mass (g) and thickness (mm) of the samples were measured. After the samples were immersed in water, the weights and thicknesses of each sample were measured at the time intervals of 1 h, 2 h, 3 h, 4 h, 5 h, 6 h, 8 h, 10 h, 20 h, and 22 h, and then every 24 h until no weight and thickness changes were observed. The surface water was removed before each measurement. The percent change in water absorption and thickness swelling was calculated using Equations (1) and (2), respectively.

$$WA(\%) = \frac{M_t - M_o}{M_o} \times 100 \quad (1)$$

where M_t is the mass at time t and Mo is the initial mass.

$$TS(\%) = \frac{T_t - T_o}{T_o} \times 100 \quad (2)$$

where T_t is the thickness at time t and T_o is the initial thickness.

Three replicates were used and averaged. A swelling and water absorption model developed by Shi and Gardner (2006) was used to predict the thickness swelling and water absorption as a function of time [18].

$$TS(\%) = \left(\frac{T_\infty}{T_0(T_\infty - T_O)e^{-K_{sr}t}} - 1 \right) \times 100 \quad (3)$$

K_{sr} is the thickness swelling rate constant and T∞ is the equilibrium thickness.

$$WA(\%) = \left(\frac{W_\infty}{W_0(W_\infty - W_O)e^{-K_{ar}t}} - 1 \right) \times 100 \quad (4)$$

K_{ar} is the water absorption rate constant and T∞ is the equilibrium weight.

Curve fitting was performed by taking the sum of square difference (SSD) between the observed and predicted data in order to fit the model to the raw data by adjusting the parameters until the minimum SSD was obtained.

$$SSD = \sum (O - P)^2 \quad (5)$$

where O are the observed data and P are the predicted data.

2.6. Differential Scanning Calorimetry (DSC)

The DSC analysis was conducted on the BFL/PLA composites using Perkin Elmer (Waltham, MA, USA) DSC 4000 with the Pyris software, in order to determine their thermal properties in regard to glass transition and crystallinity. Five samples were tested including the BFM-PLA composites (samples 1, 2, and 3). Neat PLA and raw fiber were also tested as control samples. Each sample group consisted of three replicates and were cycled 2 times.

The DSC analysis was performed at a flow rate of 20 mL min^{-1} using nitrogen gas. The mass of the samples was between 5 mg and 12 mg and the samples were placed in an aluminum sample pan. All samples were heated from 30 °C to 250 °C at a rate of 5 °C/min. Once the temperature reached 250 °C, it was held at this temperature for 5 min until it reached thermal equilibrium [19].

The samples were then cooled from 250 °C to 30 °C at a rate of 5 °C/min. Once the temperature reached 30 °C, it was held at this temperature for 5 min until it reached thermal equilibrium.

2.7. Dynamic Mechanical Analysis (DMA)

DMA is an effective technique to analyze the viscoelastic properties of the polymers. DMA testing was performed to evaluate the effect of BFM incorporation on the viscoelastic behavior of the composites. TA Instruments Discovery DMA 850 was used to characterize the storage modulus E′, loss modulus E″, and tan delta (damping factor), with the highest peak representing the glass transition temperature (Tg.) The neat PLA and BFM-PLA samples were cut to 25 mm in length, 5 mm in width, and 2 mm in thickness using a gravograph laser cutter LS100. All dry tests were carried out using a single screw film clamp. The samples were subjected to an initial load of 1 N with a control amplitude of 10.0 µm. The temperature was ramped from −20 °C to 140 °C at a rate of 2.0 K/min for dry thermomechanical testing [20].

3. Results and Discussion

After the BFM-PLA samples were compression-molded, the surface of the samples was examined. The overall penetration of the PLA resin into the hemp fiber mat is shown in Figure 3.

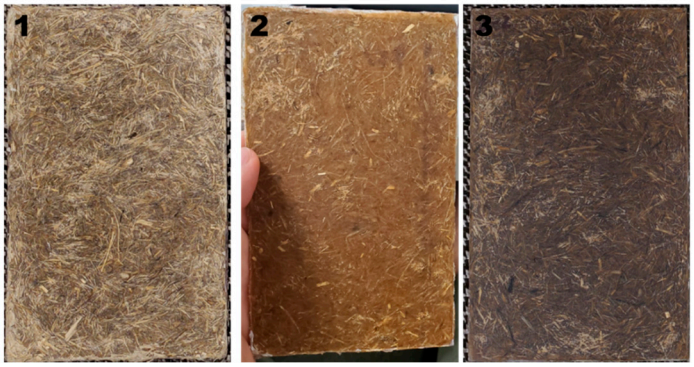

Figure 3. Surface finish of hemp/PLA samples 1–3 (Note: Sample 1: BFM/PLA 63/47; Sample 2: BFM/PLA 42/58; Sample 3: BFM/PLA 35/65).

Based on the surface finish of the samples, the initial hemp-fiber-to-PLA ratio of sample 1 did not utilize enough PLA, which resulted in hemp surface fibers not being encased in the resin. By comparing the initial fiber/PLA ratios to the final fiber/PLA ratios, the amount of PLA loss during pressing could be determined (Table 1). The fiber content of the samples increased due to PLA being squeezed out as compression pressure was increased. The lower the initial fiber content, the more PLA was lost during pressing. The higher the initial PLA content, the better the surface finish.

3.1. Mechanical Properties

Figures 4 and 5 show the bending and tensile properties of the BFM-PLA samples at different initial fiber contents.

Sample 1 possessed higher Young's modulus and modulus of elasticity (MOE) than the other BFM-PLA samples, due to its higher final BFM content. Sample 2 showed a similar Young's modulus and slightly lower MOE to those of sample 1. However, sample 1 had the best MOR and ultimate tensile strength. This can be contributed to its higher initial fiber content and better PLA penetration.

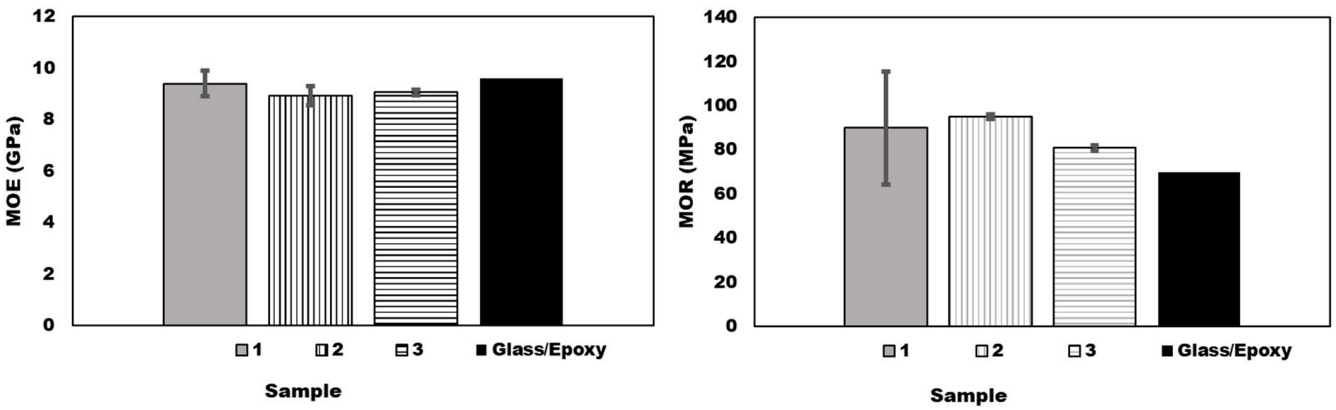

Figure 4. Bending properties: modulus of elasticity (MOE) on the left and modulus of rupture (MOR) on the right (Note: Sample 1: BFM/PLA 63/47; Sample 2: BFM/PLA 42/58; Sample 3: BFM/PLA 35/65).

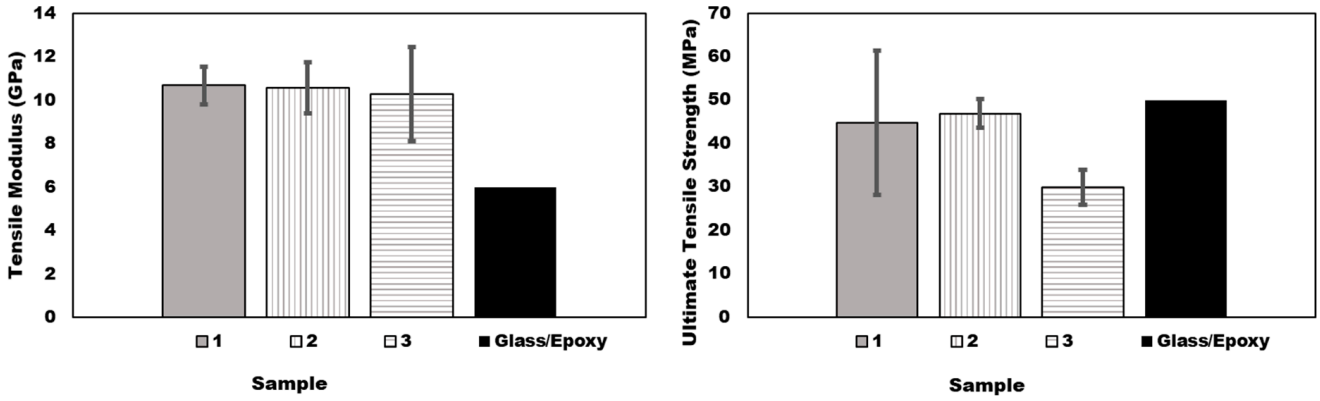

Figure 5. Tensile properties: Young's modulus on the left and ultimate tensile strength on the right (Note: Sample 1: BFM/PLA 63:47; Sample 2: BFM/PLA 42:58; Sample 3: BFM/PLA 35/65).

Based on these observations, the ratio used in sample 1 would not be suitable due to its poor surface finish. Sample 3 with a higher initial PLA content had a better surface finish, while its mechanical properties were the lowest among the three samples. Sample 2 was the best among the three formulations, and its properties were compared to the commercial glass/epoxy composites. This shows that the BFM-PLA composites have comparable mechanical properties to those of the glass/epoxy composite [21].

3.2. Hygroscopic Properties

The results of WA and TS as a function of time are shown in Figure 6.

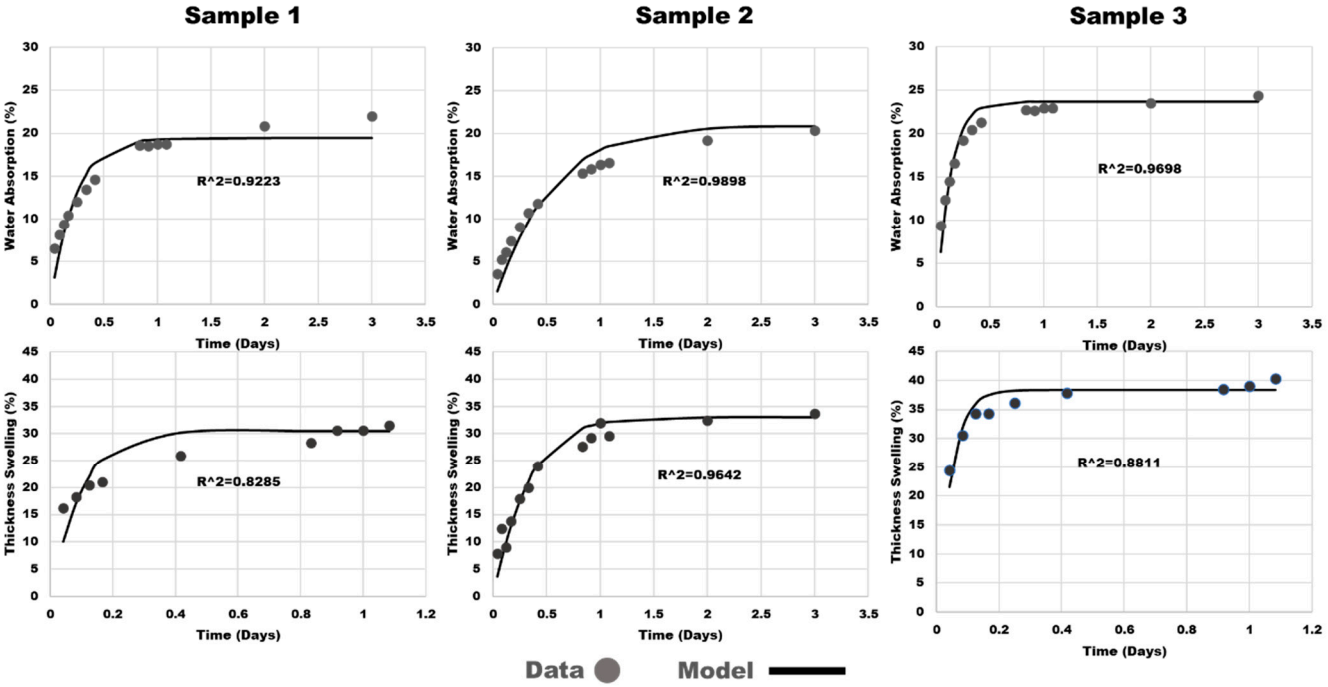

Figure 6. Water absorption properties and thickness swelling properties (Note: Sample 1: BFM/PLA 63/47; Sample 2: BFM/PLA 42:58; Sample 3: BFM/PLA 35/65).

As shown in Figure 6, the TS and WA models fit the experimental data for the hemp/PLA composite samples very well, with h R^2 values of >0.83 (Figure 7). It was observed that as the initial fiber content decreased, the water absorption and thickness swelling increased; this can be attributed to the disruption of the structural integrity during the squeeze-out of excess PLA during pressing, which would cause poorer bonding, allow-

ing for water to be trapped at the interface of the hemp fiber and PLA. Due to sample 1 (BFM/PLA 53/47) displaying the least amount of squeeze-out of PLA during pressing, it possessed the best thickness swelling and water absorption.

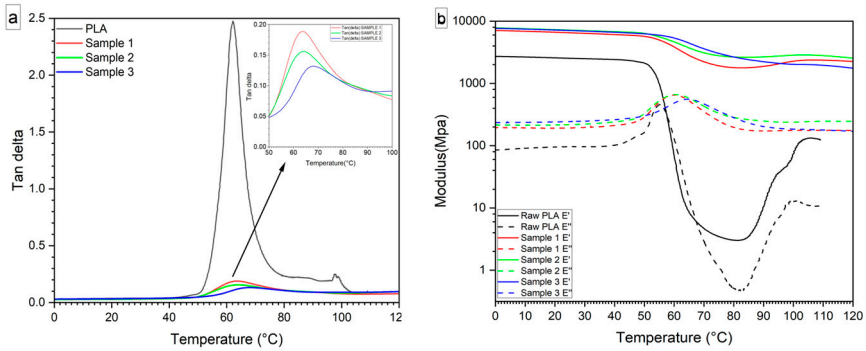

Figure 7. (**a**) Tan delta of PLA and BFM-PLA composites as a function of temperature and (**b**) storage and loss modulus of PLA and BFM-PLA composites as a function of temperature. (Note: Sample 1: BFM/PLA 63/47; Sample 2: BFM/PLA 42/58; Sample 3: BFM/PLA 35/65).

As shown in Table 2, the WA and TS rates (Kar and Ksr) for sample 2 (BFM/PLA 43/57) are significantly lower than those of samples 1 and 3 (2.17 vs. 4.92–8.79 for the WA rate and 3.65 vs. 11.84–24.56 for the thickness swelling rate), indicating that sample 2 (BFM/PLA 43/57) has much better hygroscopic dimensional stability. Sample 1 (BFM/PLA 53/47) did not have enough PLA to cover the BFM to allow for better bonding between the BFM and PLA, which can be seen in the surface coloration of sample 1 (BFM/PLA 53/47) in Figure 3. For sample 3 (BFM/PLA 35/65), too much PLA squeezed out during pressing, which disrupted the structure of the composites. By comparing the hygroscopic properties to the mechanical properties of the samples, it can be seen that the disruption in sample 3 (BFM/PLA 35/65) from the squeeze-out of PLA played a role in both sets of properties. As for sample 1 (BFM/PLA 53/47), its lower PLA content helped to minimize PLA squeeze-out, which allowed for the sample to have less disruption of the BFM, allowing for higher mechanical properties than sample 3 (BFM/PLA 35/65) but not as high as those of sample 2 (BFM/PLA 43/57) which had enough of the BFM covered by PLA.

Table 2. Water absorption and thickness swelling parameters.

	Absorption Parameters		**Swelling Parameters**	
Sample	Kar	R^2	Ksr	R^2
1 (BFM/PLA 53/47)	4.92	0.92	11.84	0.83
2 (BFM/PLA 43/57)	2.17	0.99	3.65	0.96
3 (BFM/PLA 35/65)	8.79	0.97	24.56	0.88

3.3. DSC Analysis

The DSC of the BFM-PLA composites and the raw PLA showed three peaks at specific temperatures: the glass transition temperature (T_g), the crystallization temperate (T_c), and the melting temperature (T_m) (Table 3) [22].

Table 3. DSC data for BFM/PLA composites.

Sample	**T_g (°C)**	**T_c (°C)**	**T_m (°C)**
PLA	63.56	111.46	150.83
1 (BFM/PLA 53/47)	65.32	106.08	158.27
2 (BFM/PLA 43/57)	65.43	110.90	156.14
3 (BFM/PLA 35/65)	65.00	103.07	157.43

Compared to the pure PLA sample, the BFM/PLA samples show increased Tg and Tm but decreased Tc. The increase in Tg and Tm may be partially due to the addition of hemp fiber, which has more resistivity to heating. The Tc decreases for the BFM-PLA samples would be due to a blockage when the PLA attempted to recrystallize post-heating, instead of serving as nucleation points for crystallization, which re-confirms the claims made by Celick et al. [23]. They concluded that the addition of hemp fibers to PLA generally increases Tg and Tm. This is attributed to the thermal resistivity of hemp fibers, which enhances the composite's ability to withstand heat [Celick et al.], likely due to the fibers acting as physical barriers during recrystallization rather than serving as nucleation sites [23]. Stelea et al. [19] reasoned that hemp fibers' thermal resistivity stems from their lignocellulosic structure, which degrades at higher temperatures, compared to the PLA's matrix contributing to the observed increase in Tg and Tm.

As shown in studies [10,12,13], with hemp content increasing from 10% to 30%, Tc is seen to decrease. Our result is consistent with the previously published data.

3.4. DMA

DMA was conducted on the BFM-PLA composites and the raw PLA. The glass transition temperature (Tg), Tan δ peak, storage, and loss modulus at 23 °C were obtained and are shown in Table 4.

Table 4. DMA results.

Sample	Tg at Tan δ Peak (°C)	Tan δ Peak	Storage Modulus at 23 °C
PLA	62.46	2.5218	2714
1 (BFM/PLA 53/47)	63.79	0.2160	6216
2 (BFM/PLA 43/57)	64.16	0.1493	7967
3 (BFM/PLA 35/65)	68.06	0.1353	7876

The influence of hemp fiber content on storage and loss modulus and on tan delta at various temperatures is plotted in Figure 7a,b.

It was observed that the storage modulus of all composites increased from 2700 MPa to 7700 MPa with the addition of hemp fibers to PLA. Figure 7b indicates that the storage moduli of the PLA and BFM-PLA composites remains constant at temperatures below the glass transition temperature (up to around 60 °C) and subsequently decline at T_g [24]. Sample 2 (BFM/PLA 43/57), with an equal amount of PLA and fiber in the final ratio, has a higher storage modulus [11,25].

Figure 7b represents the tan delta of PLA and BFM-PLA composites as a function of temperature. The inclusion of hemp fiber reduced the area under the tan delta curve, lowering the composites' damping capabilities [26]. Also, the top of the tan delta curve is in the same temperature range, implying that the composites' glass transition temperature remains constant. Moreover, sample 3 (BFM/PLA 35/65) has a higher glass transition temperature (tan δ) due to the presence of a higher amount of PLA in it [11].

4. Conclusions

A 100% biodegradable hemp BFM/PLA composite material was successfully fabricated. The physical and mechanical properties of the BFM/PLA composites were evaluated to see the effect of the fiber-to-PLA ratios. DSC and DMA were conducted on the samples for the thermal properties of the composites. It was concluded that the optimized BFM-to-PLA ratio for the composites was 50/50. The higher fiber content led to a decrease in the crystallization temperature of the BFM/PLA composites. The lower the glass transition temperature, the higher the fiber content and the greater the storage moduli of the BFM/PLA composites were found to be. BFM/PLA composites show much promise. It

was noticed that due to the hand lay-up, the BFM was not as uniform as desired. It is expected that as mat uniformity is improved, the mechanical performance of the resulting BFM-PLA composites will be further improved.

Author Contributions: Conceptualization: L.M.S. and S.Q.S.; Methodology: L.M.S., Y.F., M.G., X.W., R.K.P. and C.W.; Formal analysis and investigation: L.M.S., R.K.P., C.J., K.M. and J.A.; Writing—original draft preparation: L.M.S., R.K.P., Y.F. and C.J.; Writing—review and editing: S.Q.S., L.M.S., M.E. and C.W.; Funding acquisition: S.Q.S.; Resources: S.Q.S. and M.E.; Material preparation: L.M.S., Y.F., R.K.P., C.J., K.M. and J.A.; Supervision: S.Q.S., L.M.S. and M.E. All authors have read and agreed to the published version of the manuscript.

Funding: The project was supported by the Department of Energy through Z&S Tech LLC (DOE SBIR DE-SC0022736).

Data Availability Statement: The original contributions presented in the study are included in the article; further inquiries can be directed to the corresponding author.

Conflicts of Interest: The authors declare no conflicts of interest. Cuicui Wang was employed by the company Z&S Tech LLC. The remaining authors declare that the research was conducted in the absence of any commercial or financial relationships that could be construed as a potential conflict of interest.

References

1. Zimniewska, M. Hemp fibre properties and processing target textile: A review. *Materials* **2022**, *15*, 1901. [CrossRef]
2. Gholampour, A.; Ozbakkaloglu, T. A review of natural fiber composites: Properties, modification and processing techniques, characterization, applications. *J. Mater. Sci.* **2020**, *55*, 829–892.
3. Lee, C.H.; Khalina, A.; Lee, S.; Liu, M. A Comprehensive Review on Bast Fibre Retting Process for Optimal Performance in Fibre-Reinforced Polymer Composites. *Adv. Mater. Sci. Eng.* **2020**, *2020*, 6074063.
4. Fu, Y.; Zhang, Y.; Allen, M.S.; Shi, S.Q. Effects of Pectinase on Bacterial Succession during Hemp Retting. *Processes* **2024**, *12*, 1725. [CrossRef]
5. Fu, Y.; Gu, H.; Wu, F.; Shi, S.Q. Comparative Life Cycle Assessment of Bacterial and Thermochemical Retting of Hemp. *Materials* **2024**, *17*, 4164. [CrossRef]
6. Naser, A.Z.; Deiab, I.; Darras, B.M. Poly (lactic acid)(PLA) and polyhydroxyalkanoates (PHAs), green alternatives to petroleum-based plastics: A review. *RSC Adv.* **2021**, *11*, 17151–17196. [PubMed]
7. Niaounakis, M. *Biopolymers: Processing and Products*; William Andrew: Norwich, NY, USA, 2014.
8. Ioelovich, M. Adjustment of hydrophobic properties of cellulose materials. *Polymers* **2021**, *13*, 1241. [CrossRef]
9. Ren, Z.; Guo, R.; Bi, H.; Jia, X.; Xu, M.; Cai, L. Interfacial adhesion of polylactic acid on cellulose surface: A molecular dynamics study. *ACS Appl. Mater. Interfaces* **2019**, *12*, 3236–3244.
10. Sawpan, M.A.; Pickering, K.L.; Fernyhough, A. Improvement of mechanical performance of industrial hemp fibre reinforced polylactide biocomposites. *Compos. Part A Appl. Sci. Manuf.* **2011**, *42*, 310–319. [CrossRef]
11. Shakoor, A.; Muhammad, R.; Thomas, N.L.; Silberschmidt, V.V. Mechanical and thermal characterisation of poly (l-lactide) composites reinforced with hemp fibres. *J. Phys. Conf. Ser.* **2013**, *451*, 012010.
12. Masirek, R.; Kulinski, Z.; Chionna, D.; Piorkowska, E.; Pracella, M. Composites of poly (L-lactide) with hemp fibers: Morphology and thermal and mechanical properties. *J. Appl. Polym. Sci.* **2007**, *105*, 255–268. [CrossRef]
13. Behalek, L.; Seidl, M.; Dobransky, J. Crystallization of Polylactic Acid Composites with Banana and Hemp Fibres by Means of DSC and XRD Methods. *Appl. Mech. Mater.* **2014**, *616*, 325.
14. Antony, S.; Cherouat, A.; Montay, G. Fabrication and characterization of hemp fibre based 3D printed honeycomb sandwich structure by FDM process. *Appl. Compos. Mater.* **2020**, *27*, 935–953. [CrossRef]
15. *ASTM D3039/D3039M-00*; Standard Test Method for Tensile Properties of Polymer Matrix Composite Materials. ASTM International: West Conshohocken, PA, USA, 2000.
16. *ASTM D7264/D7264M-15*; Standard Test Method for Flexural Properties of Polymer Matrix Composite Materials. American Society of Testing Materials: West Conshohocken, PA, USA, 2015.
17. *ASTM D1037-12*; Standard Test Methods for Evaluating Properties of Wood-Base Fiber and Particle Panel Materials. American Society for Testing and Materials: West Conshohocken, PA, USA, 2020. [CrossRef]
18. Shi, S.Q.; Gardner, D.J. Hygroscopic thickness swelling rate of compression molded wood fiberboard and wood fiber/polymer composites. *Compos. Part A Appl. Sci. Manuf.* **2006**, *37*, 1276–1285.

19. Stelea, L.; Filip, I.; Lisa, G.; Ichim, M.; Drobotă, M.; Sava, C.; Mureșan, A. Characterisation of Hemp Fibres Reinforced Composites Using Thermoplastic Polymers as Matrices. *Polymers* **2022**, *14*, 481. [CrossRef] [PubMed]
20. Gupta, M.K.; Singh, R. Flexural and dynamic mechanical analysis (DMA) of polylactic acid (PLA) coated sisal fibre reinforced polyester composite. *Mater. Today Proc.* **2018**, *5*, 6109–6114.
21. Matweb. Overview of Materials for Epoxy, Molded, Glass Fiber Filler. Available online: https://www.matweb.com/search/datasheet.aspx?matguid=035d2130b7f34d918e8d590659b85cb7&ckck=1 (accessed on 28 August 2024).
22. Baghaei, B.; Skrifvars, M.; Rissanen, M.; Ramamoorthy, S.K. Mechanical and thermal characterization of compression moulded polylactic acid natural fiber composites reinforced with hemp and lyocell fibers. *J. Appl. Polym. Sci.* **2014**, *131*, 40534.
23. Celik, E.; Uysal, M.; Gumus, O.Y.; Tasdemir, C. 3D-Printed Biocomposites from Hemp Fibers Reinforced Polylactic Acid: Thermal, Morphology, and Mechanical Performance. *BioResources* **2025**, *20*, 331–356.
24. Cristea, M.; Ionita, D.; Iftime, M.M. Dynamic mechanical analysis investigations of PLA-based renewable materials: How are they useful? *Materials* **2020**, *13*, 5302. [CrossRef]
25. Yang, S.L.; Wu, Z.H.; Yang, W.; Yang, M.B. Thermal and mechanical properties of chemical crosslinked polylactide (PLA). *Polym. Test.* **2008**, *27*, 957–963. [CrossRef]
26. Chen, C.C.; Chueh, J.Y.; Tseng, H.; Huang, H.M.; Lee, S.Y. Preparation and characterization of biodegradable PLA polymeric blends. *Biomaterials* **2003**, *24*, 1167–1173. [CrossRef] [PubMed]